# Using a Radial Point Interpolation Meshless Method for the numerical simulation of the viscoplastic extrusion process

Rodrigues, D.E.S.[1,2,3], Belinha, J.[1,2], Natal Jorge, R.M.[1,4]

[1]*Institute of Mechanical Engineering and Industrial Management (INEGI)*
*Campus da FEUP, Rua Dr. Roberto Frias 400, 4200-465 PORTO, Portugal*
*drodrigues@inegi.up.pt*
[2]*Department of Mechanical Engineering, School of Engineering of the Polytechnic of Porto (ISEP)*
*Rua Dr. António Bernardino de Almeida, 431, 4200-072 PORTO, Portugal*
*job@isep.ipp.p*
[3]*Departmento de Engenharia Mecânica, Universidade de Aveiro*
*Campus Universitário de Santiago, 3810-193 Aveiro*
[4]*Departmento de Engenharia Mecânica, Faculdade de Engenharia, Universidade do Porto*
*Rua Dr. Roberto Frias, 4200-465 PORTO, Portugal*
*rnatal@fe.up.pt*

**Abstract.** In this work, an accurate and efficient meshless technique - the Radial Point Interpolation Method (RPIM) – is used to address the numerical simulation of the viscoplastic extrusion process, which is the initial phase of the Fused Filament Fabrication (FFF), an extrusion-based additive manufacturing (AM) process. Unlike the FEM, in meshless methods, there is no preestablished relationship between the nodes in the nodal mesh. Thus, the concept of 'element' is inexistent. In meshless methods, nodal discretization can be straightforwardly modified since nodes can be added or removed from the initial nodal mesh. Hence, mesh-free techniques show a particular relevance if associated with AM processes since the nodes can be distributed to match the layer-by-layer deposition of the printing process. Additionally, meshless methods have shape functions with virtually a higher order, allowing a higher continuity and reproducibility. This work combines, for the first time, the flow formulation and the heat transfer formulation in an RPIM algorithm to simulate the extrusion process of viscoplastic materials like the ones used in the FFF. The proposed algorithm is developed, implemented, and then validated for benchmark examples. The accuracy of the obtained numerical results highlights the importance of using meshless techniques in this field.

**Keywords:** Fused Filament Fabrication (FFF), Viscoplastic extrusion, flow formulation, meshless methods, Radial Point Interpolation Method (RPIM)

## 1. Introduction

Extrusion is a key-phase in some manufacturing processes like metal forming or extrusion-based Additive Manufacturing (AM) like Fused Filament Fabrication (FFF). It is a thermally driven process in which the domain is constantly changing either by phase change (solid to semi-molten material) or space-time movement of the particles inside the extruder. In this context, the numerical modeling of such a problem is a task suitable for meshless methods [1]. As their name suggests, these are advanced discretization techniques in which the problem domain is discretized using a set of nodes with no preestablished relationship – unlike the finite element method (FEM), for instance. Hence, the nodes can be arbitrarily distributed, and the velocities, pressures, and temperatures within the extrusion process are approximated using the influence-domain concept rather than an element. Therefore, the nodal discretization can be rearranged since nodes can be added or removed from the initial nodal mesh – the refinement procedure [2] becomes fairly straightforward. More importantly, since there are no initial connections between nodes, meshless methods do not face mesh distortions that would otherwise suggest the implementation of remeshing procedures. Thus, the authors understand that meshless methods have the potential to progress in many engineering applications, particularly in the numerical simulation of AM processes. Recently developed meshless methods have been studied in several applications such as crack path prediction [3], dental

implants [4], damage models [5], bone remodeling [1], static [2] and dynamic [6] analysis of composite plates and shells, micromechanical analyses [7], etc. This work investigates the advantages of using a simple meshless method, the Radial Point Interpolation Method (RPIM) [8], in the simulation of the viscoplastic extrusion process that occurs in the FFF and metal forming processes.

## 2. Radial Point Interpolation Method (RPIM)

The RPIM is an advanced version of the Point Interpolation Method (PIM) [9], which adds radial basis functions (RBF) to the polynomial basis function already used in PIM. Therefore, the shape functions in the RPIM are stabler and more robust interpolation functions than in the RPIM. In this meshless method, nodal connectivity is ensured through the overlap of the influence-domains. In two-dimensional problems, like the one analyzed in this study, influence-domains, are circular areas whose center are the integration points. The size of the area depends on the user's choice to use fixed or variable size influence-domains. Thus, influence-domains can have distinct areas but the same number of nodes within those areas – this is the preferable option since it creates shape functions with the same degree of complexity.

In the RPIM, the differential equations of the Galerkin weak form are integrated using the Gauss-Legendre quadrature creating a background integration mesh. This mesh is composed of quadrilateral cells and in each cell are placed the required Gauss integration points. Thus, this approach is similar to the FEM's integration procedure. The complete RPIM formulation is available in the literature [1], [10]. This work will now focus on the implementation of the extrusion model within an RPIM's code.

## 3. Extrusion Model and Computer Implementation

In this work, the fluid flow formulation, initially proposed by Zienkiewicz [11]–[15] is adapted from the FEM to the RPIM. The approach by Zienkiewicz and Godbole [15] is the study used in this paper as a reference since it gives a more general solution for viscoplastic materials. Some considerations are taken into account before presenting the governing equations and the discrete system of equations: (1) the extrusion process involves large deformations, so the elastic effects are generally insignificant and will be neglected [13]; (2) the latter assumption leads to the treatment of the fluids studied here as viscoplastic non-Newtonian fluids; (3) the materials are considered to be isotropic and incompressible; (4) The Reynolds number is considered to be small [16], and so flow is considered laminar.

### 3.1. Governing equations

The equilibrium equations of the extrusion process can be expressed as a system of three equations: mass conservation, momentum conservation, and energy conservation, as show in Eq. (1):

$$\begin{aligned} \nabla \cdot \boldsymbol{v} &= 0 \\ \nabla \cdot \boldsymbol{\sigma} + \boldsymbol{b} &= 0 \\ \rho c \left[ \frac{\partial T}{\partial t} + \boldsymbol{v} \left( \nabla T \right) \right] &= -\nabla \cdot \boldsymbol{q} + Q + \Phi \end{aligned} \tag{1}$$

where $\boldsymbol{\sigma} = \boldsymbol{D}\left(\dot{\boldsymbol{\varepsilon}}, T\right) \cdot \dot{\boldsymbol{\varepsilon}}$ is the stress tensor, $\boldsymbol{D}$ the constitutive matrix of the material which can be dependent on the strain rate, $\dot{\boldsymbol{\varepsilon}} = \frac{1}{2}\left[ \nabla \boldsymbol{v} + \left( \nabla \boldsymbol{v} \right)^T \right]$, and the temperature, $T$, $\boldsymbol{v}$ is velocity field, $\boldsymbol{b}$ represents the body forces, $\rho$ is the density, $c$ is the material heat capacity per unit volume, and $\nabla \cdot \boldsymbol{q}$ is the divergence of the heat flux, which is proportional to the temperature gradient following the Fourier heat conduction law:

$$\boldsymbol{q} = -\boldsymbol{k} \nabla T \tag{2}$$

where $\boldsymbol{k} = k\boldsymbol{I}$ is the thermal conductivity ($k$ is a constant for isotropic and homogeneous materials). $Q$ is the conductive heat, and $\Phi$ is the viscous dissipation [17] given by:

$$\Phi = 2\mu\dot{\varepsilon}_{ij}\dot{\varepsilon}_{ij} \tag{3}$$

Thus, the energy conservation equation can be rewritten as:

$$\rho c\left[\frac{\partial T}{\partial t} + \boldsymbol{v}\left(\nabla T\right)\right] = \nabla^T\left(\boldsymbol{k}\nabla T\right) + Q + 2\mu\dot{\boldsymbol{\varepsilon}} : \dot{\boldsymbol{\varepsilon}} \tag{4}$$

Regarding the material's constitutive behavior, for general non-Newtonian fluids, there is a strain-rate and temperature-dependent viscosity: $\mu = \mu\left(T, \dot{\bar{\varepsilon}}\right)$. However, it is common to simplify the viscosity's dependency as $\mu = \mu\left(\dot{\bar{\varepsilon}}\right)$ [18], with effective strain rate defined as $\dot{\bar{\varepsilon}} = \sqrt{\frac{2}{3}\dot{\boldsymbol{\varepsilon}} : \dot{\boldsymbol{\varepsilon}}}$. In this work, to model the material's viscosity, the Perzyna model for viscoplastic materials is used. Perzyna's viscoplastic model is dependent on three material parameters: the fluidity parameter, $\gamma$, the power coefficient $n$, and the yield stress, $\sigma_Y\left(\dot{\bar{\varepsilon}}, T\right)$:

$$\mu = \frac{\sigma_Y + \left(\dot{\bar{\varepsilon}} / \gamma\right)^{1/n}}{3\dot{\bar{\varepsilon}}} \tag{5}$$

### 3.2. Discrete system of equations

The discrete system of equations is established by writing the weak form of the governing equations (1). This procedure was presented by Costa et al. [10], [19], [20] for the first two equations in (1). In these works, the authors obtain the solutions for the flow problem (without thermal effects) using the mixed dual method. This solution method uses two distinct nodal discretizations and computes velocities and pressures as outputs of the discrete system of equations. One of the nodal meshes is used for velocities calculation and the other nodal mesh allows the pressure computation. Independent influence-domains are established for the two nodal meshes, and so the shape functions used for velocity and pressure interpolations are not equal. Despite the nodal meshes being different, they share the same background integration mesh where RPIM's integration is performed. Thus, for a given influence-domain concentric with a certain integration point, its area will contain more velocity nodes than pressure nodes. This methodology mimics a hybrid integration scheme. In this work, the same procedure is adopted to integrate the energy conservation equation. To calculate the nodal temperatures, the velocity nodal mesh is used – then, the temperature influence-domains are the same as the velocity influence-domains.

As obtained in [10], the discrete system of equations of the flow problem (velocities and pressure as field variables), is given as:

$$\begin{bmatrix} \boldsymbol{K}_v & \boldsymbol{Q} \\ \boldsymbol{Q}^{\mathrm{T}} & \boldsymbol{V} \end{bmatrix} \begin{Bmatrix} \tilde{\boldsymbol{v}} \\ \tilde{\boldsymbol{p}} \end{Bmatrix} = \begin{Bmatrix} \boldsymbol{f} \\ 0 \end{Bmatrix} \tag{6}$$

where,

$$\begin{aligned} \boldsymbol{K}_v &= \int_\Omega \boldsymbol{B}^{\mathrm{T}} \mu \mathbf{I}_0 \boldsymbol{B}\, \mathrm{d}\Omega \\ \boldsymbol{Q} &= -\int_\Omega \boldsymbol{B}^{\mathrm{T}} \mathbf{m} \boldsymbol{\varphi}_p\, \mathrm{d}\Omega \\ \boldsymbol{f} &= \int_\Omega \left(\boldsymbol{\varphi}_v\right)^{\mathrm{T}} \boldsymbol{b}\, \mathrm{d}\Omega + \int_\Gamma \left(\boldsymbol{\varphi}_v\right)^{\mathrm{T}} \bar{\boldsymbol{t}}\, \mathrm{d}\Gamma \\ \boldsymbol{Q}^{\mathrm{T}}\tilde{\boldsymbol{v}} &- \frac{1}{\beta}\boldsymbol{V}\, \tilde{\boldsymbol{p}} = 0 \\ \boldsymbol{V} &= -\int_\Omega \left(\boldsymbol{\varphi}_p\right)^{\mathrm{T}} \boldsymbol{\varphi}_p\, \mathrm{d}\Omega \end{aligned} \tag{7}$$

$\Gamma \in \Omega$ is the traction boundary at which the external forces, $\bar{\boldsymbol{t}}$, are applied, $\tilde{\boldsymbol{v}}$ is the velocity vector containing the nodal velocities of each node composing a domain of influence with $n$ nodes, $\tilde{\boldsymbol{p}}$ is the pressure nodal vector, $\boldsymbol{\varphi}_v$ is the matrix containing the velocity interpolation functions, $\boldsymbol{\varphi}_p$ the vector containing the pressure shape functions, calculated based on the pressure influence-domains. $\boldsymbol{B}(\boldsymbol{x}_I)$ is deformation or strain matrix, containing the partial derivatives of the velocity shape functions , $\mathbf{m} = \{1 \;\; 1 \;\; 1 \;\; 0\}^{\mathrm{T}}$, $\beta = 10^{7-8}\mu$ represents a very large number enforcing the incompressibility condition, and $\mathbf{I}_0$ is presented in Eq. (8):

$$\mathbf{I}_0 = \begin{bmatrix} 2 & 0 & 0 & 0 \\ 0 & 2 & 0 & 0 \\ 0 & 0 & 2 & 0 \\ 0 & 0 & 0 & 1 \end{bmatrix} \tag{8}$$

As stated before, the discretization of the energy equation follows the same procedure described in the literature [10] for the continuity/mass-momentum equations. The temperature at $\boldsymbol{x}_I$ , $T(\boldsymbol{x}_I)$ , can be calculated using:

$$T(\boldsymbol{x}_I) = \boldsymbol{\varphi}_t(\boldsymbol{x}_I)\tilde{\boldsymbol{T}} = \left[\varphi_{t1}(\boldsymbol{x}_I) \;\; \varphi_{t2}(\boldsymbol{x}_I) \;\cdots\; \varphi_{tl}(\boldsymbol{x}_I)\right]\tilde{\boldsymbol{T}} \tag{9}$$

being $\tilde{\boldsymbol{T}} = \left\{\tilde{T}_1 \;\; \tilde{T}_2 \;\; \cdots \;\; \tilde{T}_l\right\}^{\mathrm{T}}$ the local temperature vector and $\boldsymbol{\varphi}_t$ the vector containing interpolation functions used to interpolate the temperature, calculated based on the temperature influence-domains with $l$ nodes. In this work, $\boldsymbol{\varphi}_t = \boldsymbol{\varphi}_v$. The discrete form [13], [21] of the energy conservation equation can be rewritten as:

$$\begin{aligned} &\rho c\dot{\tilde{\boldsymbol{T}}} + \int_{\Omega} \rho c \left[ \boldsymbol{\varphi}_t^{\mathrm{T}} \left( v_x \frac{\partial \boldsymbol{\varphi}_t}{\partial x} \right) + \boldsymbol{\varphi}_t^{\mathrm{T}} \left( v_y \frac{\partial \boldsymbol{\varphi}_t}{\partial y} \right) \right] \mathrm{d}\Omega \tilde{\boldsymbol{T}} - \\ &- \int_{\Omega} k \left[ \left( \frac{\partial \boldsymbol{\varphi}_t}{\partial x} \right)^{\mathrm{T}} \left( \frac{\partial \boldsymbol{\varphi}_t}{\partial x} \right) + \left( \frac{\partial \boldsymbol{\varphi}_t}{\partial y} \right)^{\mathrm{T}} \left( \frac{\partial \boldsymbol{\varphi}_t}{\partial y} \right) \right] \mathrm{d}\Omega \tilde{\boldsymbol{T}} = \int_{\Omega} \left(\boldsymbol{\varphi}_t\right)^{\mathrm{T}} \Phi \; \mathrm{d}\Omega + \int_{\Gamma} \left(\boldsymbol{\varphi}_t\right)^{\mathrm{T}} Q \, \mathrm{d}\Gamma \end{aligned} \tag{10}$$

where $\dot{\tilde{\boldsymbol{T}}}$ the temperature derivative with respect to time. The previous equation can be condensed in the following manner, for a bidimensional problem:

$$\rho c\dot{\tilde{\boldsymbol{T}}} + \left[ \int_{\Omega} \rho c \, \boldsymbol{\varphi}_t \left\{ v_x \quad v_y \right\} \boldsymbol{B}_t \, \mathrm{d}\Omega - \int_{\Omega} \boldsymbol{B}_t^{\mathrm{T}} k \, \boldsymbol{B}_t \, \mathrm{d}\Omega \right] \tilde{\boldsymbol{T}} = \int_{\Omega} \left(\boldsymbol{\varphi}_t\right)^{\mathrm{T}} \Phi \; \mathrm{d}\Omega + \int_{\Gamma} \left(\boldsymbol{\varphi}_t\right)^{\mathrm{T}} Q \, \mathrm{d}\Gamma \tag{11}$$

with,

$$\boldsymbol{B}_t = \begin{bmatrix} \dfrac{\partial \varphi_{t1}}{\partial x} & \dfrac{\partial \varphi_{t2}}{\partial x} & \cdots & \dfrac{\partial \varphi_{tl}}{\partial x} \\ \dfrac{\partial \varphi_{t1}}{\partial y} & \dfrac{\partial \varphi_{t2}}{\partial y} & \cdots & \dfrac{\partial \varphi_{tl}}{\partial y} \end{bmatrix} \tag{12}$$

Equation (12) expresses a transient problem in time which is solved here using a backward finite difference to obtain the time derivatives:

$$\dot{\tilde{\boldsymbol{T}}} = \frac{\mathrm{d}\tilde{\boldsymbol{T}}}{\mathrm{d}t} = \frac{\tilde{\boldsymbol{T}}^{t} - \tilde{\boldsymbol{T}}^{t-\Delta t}}{\Delta t} \tag{13}$$

$\Delta t$ is a time-step, $\tilde{\boldsymbol{T}}^{t}$ is temperature field of the present time-step, and $\tilde{\boldsymbol{T}}^{t-\Delta t}$ the temperature vector of the previous time-step. Thus, the discrete system of equations of the heat transfer problem is finally given as:

$$\left(\boldsymbol{D}+\boldsymbol{L}+\boldsymbol{M}\right)\tilde{\boldsymbol{T}}=\boldsymbol{g}+\frac{\rho c}{\Delta t}\tilde{\boldsymbol{T}}^{t-\Delta t} \tag{14}$$

where,

$$\begin{aligned}\boldsymbol{D}&=\int_{\Omega}\rho c\,\boldsymbol{\varphi}_t\left\{v_x \quad v_y\right\}\boldsymbol{B}_t\,\mathrm{d}\Omega\\ \boldsymbol{L}&=-\int_{\Omega}\boldsymbol{B}_t^{\mathrm{T}}k\,\boldsymbol{B}_t\,\mathrm{d}\Omega\\ \boldsymbol{M}&=\frac{\rho c}{\Delta t}\mathbf{I}\\ \boldsymbol{g}&=\int_{\Omega}\left(\boldsymbol{\varphi}_t\right)^{\mathrm{T}}\Phi\,\mathrm{d}\Omega+\int_{\Gamma}\left(\boldsymbol{\varphi}_t\right)^{\mathrm{T}}Q\,\mathrm{d}\Gamma\end{aligned} \tag{15}$$

$\mathbf{I}$ is an identity tensor with dimensions $[l\times l]$, $\boldsymbol{D}$ is the convective or transport matrix, $\boldsymbol{L}$ is the thermal conductivity matrix, and $\boldsymbol{g}$ is the heat loading vector. Under steady-state conditions, the system (14) becomes:

$$\left(\boldsymbol{D}+\boldsymbol{L}\right)\tilde{\boldsymbol{T}}=\boldsymbol{g} \tag{16}$$

Finally, the complete discrete system of equations is given in Eq. (17):

$$\begin{aligned}&\begin{bmatrix}\boldsymbol{K}_v & \boldsymbol{Q}\\ \boldsymbol{Q} & \boldsymbol{V}\end{bmatrix}\begin{Bmatrix}\tilde{\boldsymbol{v}}\\ \tilde{\boldsymbol{p}}\end{Bmatrix}=\begin{Bmatrix}\boldsymbol{f}\\ 0\end{Bmatrix}\\ &\left(\boldsymbol{D}+\boldsymbol{L}\right)\tilde{\boldsymbol{T}}=\boldsymbol{g}\end{aligned} \tag{17}$$

The implemented uncoupled/sequential algorithm solves first the first system of equations in (17) – the mass-momentum equations – and then solves the energy equations to compute the temperature field iteratively, since the temperature is velocity-dependent.

## 4. Preliminary Numerical Results

The system of equations attained in the last section, combined with the RPIM formulation, derives into an algorithm capable to simulate the viscoplastic extrusion process. To do so, it is required to define the Perzyna's material parameters $\sigma_Y$, $\gamma$, and $n$ - which are found in [13], [22] as a function of the temperature (given in ºF) for a titanium alloy, Ti-6Al-4V, the same material studied by Zienkiewicz et al. in [13]. The problem domain is described in Fig. 1. At the bottom boundary, a symmetry condition is imposed, while at the left boundary, a velocity of $v_x = 3.5\ \mathrm{cm/s}$ and a temperature of $T = 1750\,^{\circ}\mathrm{F}$ are imposed. In the RPIM formulation, a regular nodal mesh with 3817 nodes was created, composed of 180 grid divisions in the horizontal direction and 36 divisions in the vertical direction. 6 by 6 Gaussian integration points were considered for each grid division and the velocity and temperature influence-domains are composed of 16 nodes.

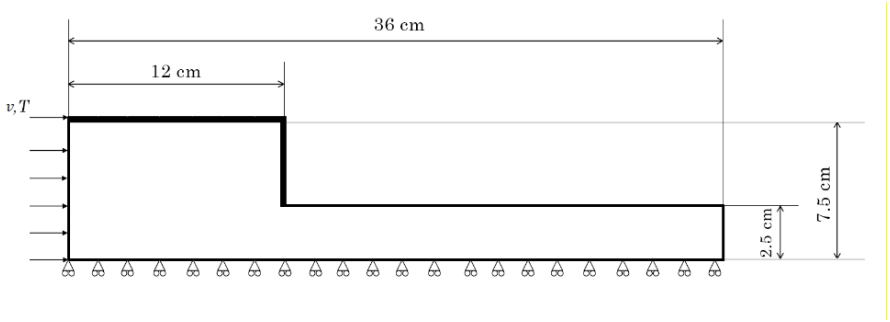


Figure 1 - Plane extrusion model domain.

Figure 2 shows the results obtained with the RPIM/mixed dual method for a steady-state plane viscoplastic extrusion problem. The graphs of Fig. 2 took 4 iterations to be computed, which shows fast convergence of the meshless approach for this highly nonlinear problem.

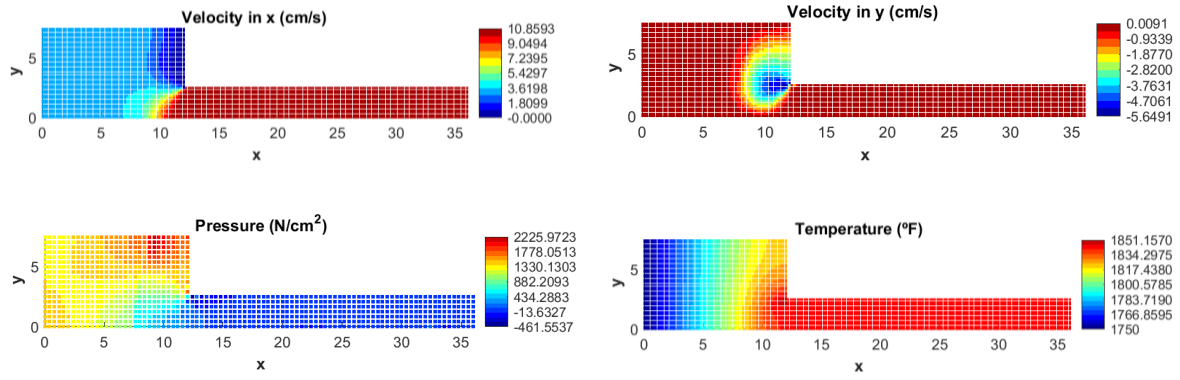


Figure 2 – Velocities ( $\mathrm{cm/s}$ ), pressure ( $\mathrm{N/cm^2}$ ), and temperature ( $^{\circ}\mathrm{F}$ ) fields for the plane extrusion benchmark problem.

The temperature map in Fig. 2 is smooth and physically reasonable: higher temperature spots are subjected to higher velocities, which generates higher strain rates and therefore an increase in viscous dissipation. In [13], Zienkiewicz et al. provides a very similar graph for the temperature field but computed using the FEM with nine-noded isoparametric Lagrangian quadrilateral elements with biquadratic shape functions for velocities and temperature. Comparing both graphs, it can be found that the relative difference between the maximum temperature computed with the RPIM/mixed dual method and the maximum temperature obtained using the high-order FEM [13] is 0.47%, since the highest computed temperature with the RPIM is 1851.12 ºF and in [13] the maximum obtained temperature is 1860 ºF. Zienkiewicz et al. did not present velocity and pressure maps so the same comparison cannot be performed for the other variables.

## Conclusions

The RPIM was used as a discretization technique to compute the integrodifferential equations obtained from the Galerkin weak form applied to a fluid flow/heat transfer problem. Therefore, the developed algorithm, here briefly explained, can be used to simulate the extrusion process on viscoplastic materials, In the implemented algorithm, the temperature field depends on the velocity field, which then depends on the material viscosity which is temperature and strain rate-dependent, making this a highly non-linear problem. The RPIM proved to be a capable and efficient method to study the uncoupled flow and heat transfer problem, achieving similar results to high-order FEM and not facing mesh distortions due to its meshfree characteristic.

Analyzing the preliminary results of this study, the new algorithm can be capable of future analyzing the viscoplastic extrusion process applied to metal forming processes or AM processes, once the viscoplastic material parameters are known.

**Acknowledgements.** The authors truly acknowledge the funding provided by Ministério da Ciência, Tecnologia e Ensino Superior – Fundação para a Ciência e a Tecnologia (Portugal), under grant SFRH/BD/121019/2016, and by project funding MIT-EXPL/ISF/0084/2017. Additionally, the authors acknowledge the funding provided by the Fulbright Commission – AY 2019/20.

**Authorship statement.** The authors hereby confirm that they are the sole liable persons responsible for the authorship of this work, and that all material that has been herein included as part of the present paper is either the property (and authorship) of the authors or has the permission of the owners to be included here.

## References


[1] J. Belinha, *Meshless Methods in Biomechanics: Bone Tissue Remodelling Analysis*. Porto: Springer International Publishing, 2014.

[2] J. Belinha, A. L. Araújo, A. J. M. Ferreira, L. M. J. S. Dinis, and R. M. N. Jorge, "The analysis of laminated plates using distinct advanced discretization meshless techniques," *Compos. Struct.*, vol. 143, pp. 165–179, 2016, doi: 10.1016/j.compstruct.2016.02.021.

[3] J. M. C. Azevedo, J. Belinha, L. M. J. S. Dinis, and R. M. Natal Jorge, "Crack path prediction using the natural neighbour radial point interpolation method," *Eng. Anal. Bound. Elem.*, vol. 59, pp. 144–158, 2015, doi: 10.1016/j.enganabound.2015.06.001.

[4] H. M. S. Duarte, J. R. Andrade, L. M. J. S. Dinis, R. M. N. Jorge, and J. Belinha, "Numerical analysis of dental implants using a new advanced discretization technique," *Mech. Adv. Mater. Struct.*, vol. 23, no. 4, pp. 467–479, 2015, doi: 10.1080/15376494.2014.987410.

[5] B. V Farahani, J. Belinha, F. M. Andrade Pires, A. J. M. Ferreira, and P. M. G. P. Moreira, "Extending a radial point interpolation meshless method to non-local constitutive damage models," *Theor. Appl. Fract. Mech.*, vol. 85, Part A, pp. 84–98, Oct. 2016, doi: http://dx.doi.org/10.1016/j.tafmec.2016.08.008.

[6] H.-H. Phan-Dao, "A Meshfree Radial Point Interpolation Method for Free Vibration of Laminated Composite Plates Analysis Based on Layerwise Theory," *Procedia Eng.*, vol. 142, pp. 349–356, 2016, doi: 10.1016/j.proeng.2016.02.061.

[7] R. Wang *et al.*, "A novel approach to impose periodic boundary condition on braided composite RVE model based on RPIM," *Compos. Struct.*, vol. 163, no. Supplement C, pp. 77–88, 2017, doi: https://doi.org/10.1016/j.compstruct.2016.12.032.

[8] J. G. Wang and G. R. Liu, "A point interpolation meshless method based on radial basis functions," *Int. J. Numer. Methods Eng.*, vol. 54, no. 11, pp. 1623–1648, 2002.

[9] G. R. Liu and Y. T. Gu, "A point interpolation method for two-dimensional solids," *Int. J. Numer. Methods Eng.*, vol. 50, no. 4, pp. 937–951, 2001.

[10] R. O. S. S. Costa, J. Belinha, R. M. N. Jorge, and D. E. S. Rodrigues, "OPTIMIZING A MESHLESS METHOD FOR THE SIMULATION OF THE EXTRUSION OF NON-NEWTONIAN MATERIALS," *Int. J. Mech. Sci.*, p. 106688, 2021, doi: 10.1016/j.ijmecsci.2021.106688.

[11] O. C. Zienkiewicz, "Flow formulation for numerical solution of forming processes," *Numer. Anal. Form. Process.*, vol. 25, pp. 1–44, 1984.

[12] P. Zienkiewicz, O. C., Taylor, R.L. Nithiarasu, *The Finite Element Method for Fluid Dynamics*, 7th ed. Waltham, MA: Butterworth-Heinemann, 2013.

[13] O. C. Zienkiewicz, E. Oñae, and J. C. Heinrich, "A general formulation for coupled thermal flow of metals using finite elements," *Int. J. Numer. Methods Eng.*, vol. 17, no. 10, pp. 1497–1514, 1981, doi: 10.1002/nme.1620171005.

[14] O. C. Zienkiewicz, P. C. Jain, and E. Onate, "Flow of solids during forming and extrusion: Some aspects of numerical solutions," *Int. J. Solids Struct.*, vol. 14, no. 1, pp. 15–38, 1978, doi: 10.1016/0020-7683(78)90062-8.

[15] O. C. Zienkiewicz and P. N. Godbole, "Flow of plastic and visco-plastic solids with special reference to extrusion and forming processes," *Int. J. Numer. Methods Eng.*, vol. 8, no. 1, pp. 1–16, 1974, doi: 10.1002/nme.1620080102.

[16] M. P. Serdeczny, R. Comminal, M. T. Mollah, D. B. Pedersen, and J. Spangenberg, "Numerical modeling of the polymer flow through the hot-end in filament-based material extrusion additive manufacturing," *Addit. Manuf.*, vol. 36, p. 101454, 2020, doi: https://doi.org/10.1016/j.addma.2020.101454.

[17] S. S. Rao, "Chapter 17 - Basic Equations of Fluid Mechanics," S. S. B. T.-T. F. E. M. in E. (Fifth E. Rao, Ed. Boston: Butterworth-Heinemann, 2011, pp. 549–569.

[18] O. C. Zienkiewicz and R. L. Taylor, "Chapter 4 - Incompressible laminar flow - newtonian and non-newtonian fluids," in *The Finite Element Method, Volume 3: Fluid Dynamics*, 5th ed., Woburn, MA: Butterworth-Heinemann, 2000, pp. 91–142.

[19] R. Costa, J. Belinha, and R. Natal Jorge, "The extension of a radial point interpolation meshless method to the viscoplastic extrusion process," Faculty of Engineering of University of Porto, 2018.

[20] R. Costa, J. Belinha, R. M. Natal Jorge, and D. E. S. Rodrigues, "Simulation of the viscoplastic extrusion process using the radial point interpolation meshless method," *Proc. Inst. Mech. Eng. Part L J. Mater. Des. Appl.*, p. 1464420720988583, Jan. 2021, doi: 10.1177/1464420720988583.

[21] K. H. Huebner, D. L. Dewhirst, D. E. Smith, and T. G. Byrom, *The Finite Element Method for Engineers*, vol. 6: Elastic. Wiley, 2001.

[22] A. U. Sulijoadikusumo and O. W. Dillon, "Work Softening of Ti-6A1-4V Due to Adiabatic Heating," in *Metallurgical Effects at High Strain Rates*, R. W. Rohde, B. M. Butcher, J. R. Holland, and C. H. Karnes, Eds. Boston, MA: Springer US, 1973, pp. 501–518.